Journal of Applied Polymer Science

Rapid polymer fiber airbrushing: Impact of a device design on the fiber fabrication and matrix quality

Wojtek Tutak, Grant Gelven, Chris Markle, Xavier-Lewis Palmer
ADA Foundation, Dr. Anthony Volpe Research Center, Gaithersburg, Maryland
Correspondence to: W. Tutak (E-mail: wojtek.tutak@nist.gov)

ABSTRACT: Polymer fiber matrixes can be used in a variety of applications, including electronics, tissue engineering, or coatings. Polymer airbrushing (air-blast spinning) has the potential to overcome some of the limitations of electrospinning and has the advantage of depositing nanofibers directly on various materials. The airbrushing technique has yet to be better evaluated and optimized to achieve a higher fiber reproducibility and bulk material quality. In this study, a gravity-fed brush (commercial airbrush) and syringe-pump-operated brush [custom-built airbrush (CBA)] were compared to determine the effect of the coaxial brush design on the efficacy of fiber fabrication. At comparable fiber deposition rates, gas pressures, and polymer concentrations, the CBA produced smaller and more uniform fibers with a lower average size of polymer beads. The obtained data suggest that capillary pinching was the dominant mechanism responsible for fiber formation when we used the CBA. The estimated pinching energy was lower for the CBA at the compared polymer concentrations and at a high gas pressure. © 2015 Wiley Periodicals, Inc. J. Appl. Polym. Sci. **2015**, *132*, 42813.

KEYWORDS: biomaterials; biomedical applications; biomimetic; electrospinning; fibers

Received 17 February 2015; accepted 4 August 2015
DOI: 10.1002/app.42813

INTRODUCTION

Polymer fibers with a submicrometer size, high aspect ratio, and adjustable chemical composition are desirable for many engineering applications. Single fibers may have a high strength[1,2] and good thermal and electrical conductivity,[3–6] form band-gap transistors,[7,8] or have high bioactivity.[9] Polymer fibers can also form matrices that may be applied to coat large areas for applications, including biointerface layers on implants, antifouling coatings for marine applications, or large-area wearable antennas.[10–12] The improvement of fiber fabrication is vital for controlling single-fiber and bulk film quality, for engineering applications, and to ensure reproducible mechanical, electrochemical, and biological performance. Reproducible fiber fabrication with a high fabrication rate will allow better control of bulk material properties, including the material diffusion rate, strength, surface energy, and on a single fiber level, uniform energy dissipation.[13–16]

Existing literature indicates that submicrometer fiber fabrication can be achieved with commercially available airbrushes[10,17,18] or custom-built ones.[19,20] Both designs allow for rapid nanofiber fabrication but also appear to have unique advantages and disadvantages. The design configuration, fluid chamber dimensions, and type of material used may all have an impact on the polymer solution/device feed rate, mixing, and fiber formation because of material interactions on a molecular scale.[21,22] Our previous work, as well as that of others, has shown that various polymers can form fibers with a commercial airbrush (CA).[10,17,18,23] However, these nanofibers are often formed within a limited polymer concentration range,[10,17] at high gas pressures,[24] or with the aid of chemical modifiers.[18] On the other hand, custom-built devices appear to offer better ability to control material fabrication. Oliveira *et al.*,[19] for example, successfully used an air-blast design to synthesize fibers from a range of polymer solutions.

In this study, two differently configured coaxial designs were examined to determine which design was better for fiber fabrication and why that specific design was better. A gravity-fed CA and a custom-built airbrush (CBA) connected to a syringe pump (to control the polymer feed rate) were evaluated. We hypothesized that differences in the brush design (nozzle configuration and mode of polymer feed) would have an effect on the resulting fiber diameter and matrix quality.

EXPERIMENTAL

Materials

Solutions of 2, 4, 6, and 8% w/w poly(ε-caprolactone) (PCL; 80,000 Da, Sigma Aldrich) in chloroform (Sigma Aldrich) were prepared and tested at 34.47 and 172.38 kPa (5 and 25 PSI) of air (Supporting Information, Table S1). The gas pressure was

Additional Supporting Information may be found in the online version of this article

measured with a USG pressure gauge (pressure range = 0–1379 kPa) mounted on a Victor gas reducer. The air flow was controlled with a Cole–Parmer air-flow meter. Solutions ranging from 2 to 8% w/w PCL were used to test the CA, whereas solutions with 4 and 8% w/w were tested in the CBA. Because of the design limitations of the CA (gravity-fed polymer solution), an 8% w/w PCL polymer concentration was used as the maximum effective concentration.

The CA (Master Airbrush, G222-SET) was fitted with a 0.5-mm nozzle and accompanied by a guided needle. During fiber fabrication, the needle was fully withdrawn, and the nozzle adapter was removed to allow for the highest polymer solution flow.

The design of the CBA was inspired by a layout outlined in a publication by Medeiros *et al.*[20] Our design featured a slightly higher ratio between the inner and outer nozzle diameters [0.5; Supporting Information, Figures S1(a) and S2(a)]. The design and device dimensions were dictated, in part, by limitations in the machining of the aluminum alloy. A glass tube (outer diameter = 0.95 mm) was centered in the middle of the device, threaded through the nozzle (protruding 1–2 mm), and sealed in the back to prevent gas escape [Supporting Information, Figure S1(a)]. Polymer nanofibers were deposited with a syringe pump (NE 1000 X, New Era System, Inc., Farmingdale, NY) at a feed rate of 5–35 mL/h and pressures of 5 and 25 PSI for the 4 and 8% PCL solutions, respectively.

Methods

The CA delivered on an average of 12.03 mg/s fibers from a 4% w/w polymer solution at 172.37 kPa. Under comparable conditions and at a 35 mL/h polymer flow rate, the CBA produced nanofibers at a rate of 11.17 mg/s. The polymer deposition rates at 4% w/w for both designs were, therefore, deemed comparable. Testing was further extended to an 8% w/w polymer concentration (the highest possible for CA).

Fiber Collection and Material Analysis. All of the polymer nanofiber specimens were collected on aluminum foil sheets or polyester mesh 15–20 cm away from the tip of the nozzle. A single mat was deposited for each tested condition. After deposition, random pieces of the nanofiber mats were analyzed with a scanning electron microscope (JEOL) at magnifications of 200× (imaged area = 0.263 mm^2) and 1500× [imaged area = 0.0046 mm^2 for fiber diameter; Supporting Information, Figure S2(b)]. All of the calculated values (except for the fiber diameter) are reported as an average over the random sample area (3.15 mm^2). The polymer fiber diameters were measured on the basis of $n \geq 15$ for each imaged area. The micrographs were analyzed with ImageJ software (NIH). The scale was adjusted before each image analysis. The operator identified the fibers/beads and then manually traced the shape outlines to calculate the diameter/area. The collected data were exported to Excel and analyzed by OriginPro software.

Viscosity Measurements. A sealed microcapillary viscometer was used to measure small polymer samples (3 μL rate sweep) within a 1–2000 viscosity (mPa s) range at room temperature.[25]

Data Analysis and Statistics. G*Power 3.0.10 software was used to carry out *post hoc* power analysis to calculate the power (at least 0.8) for the analyzed samples ($\alpha = 0.05$).[26] A one-way analysis of variance with a Tukey extension test (OriginPro software) was applied to the data with a normal distribution profile. The significance level was set at $p = 0.05$.

The excessively large beads (outliers that covered 40% or more of the image area) were excluded from analysis as they were likely caused by the operator's handling of the devices and the collecting samples. The fibers that were fused (melted) together and formed large bundles were excluded from the fiber diameter analysis. Only single fibers were analyzed. The calculated average bead areas for the CA and CBA are summarized in the Supporting Information in Table S2. Analysis for Figure 5(a–f) (nanofiber diameter) was based on data sets summarized in Supporting Information in Table S3.

The measurement of the linear correlation and slope (a) of the line analysis for Figures 2(a,b,f), 4(e,f), and 5(a–f) was carried out to highlight overall trends. The fiber diameter frequency distribution, means, and standard deviations (Figures 6 and 7) were calculated to complement the data in Figure 5(a–f).

When we estimated the energy required to pinch off fibers, the following assumptions were made: (1) a cylinder was a good approximation for the fiber shape, (2) a linear stability analysis was used to find the maximum aspect ratio achievable for a fiber, and (3) the maximum length of a fiber was determined to be about 1 mm.[27]

RESULTS

Effects of the Gas Pressure, Polymer Concentration, and Device Type on the Polymer Bead Area

Both airbrushes successfully delivered micrometer and submicrometer fibers [Figure 1(a–h)]. Larger unprocessed polymer beads were more often spotted in the CA-synthesized mats than in the CBA ones. The beads appeared to be larger on the samples collected from the CA and at higher polymer concentrations.

Initial microscopic analysis of the CA specimens revealed that the number of beads increased as the polymer concentration increased [Figure 1(a–d)]. Conversely, the nanofiber mats synthesized with the CBA did not show similar results [Figure 1(e–h)]. This initial observation prompted a more in-depth investigation, which is described later.

When the CA was used [Figure 2(a)], a positive linear correlation existed between the average counted bead area and polymer concentration (for 34.47 kPa, $R^2 = 0.96$, and for 172.37 kPa, $R^2 = 0.96$). However, for the CBA [Figure 2(b)], such a correlation existed only for fibers deposited from an 8% w/w polymer solution at 172.37 kPa ($R^2 = 0.98$). For other conditions, no clear trends were apparent. A direct comparison between the CA and CBA indicated that the average bead areas at the tested polymer concentrations and gas pressures (Figure 3 and Supporting Information, Table S2) were, on average, lower in samples synthesized with the CBA.

The number of beads in the CA samples was not dependent on the polymer concentration [Figure 4(a,b)]. Similarly, a poor correlation was found in the CBA fibers deposited at 34.47 kPa for both polymer concentrations [Figure 4(c–f)]. Interestingly, at a higher air pressure and 4% w/w PCL concentration, the polymer bead count apparently decreased with the increasing

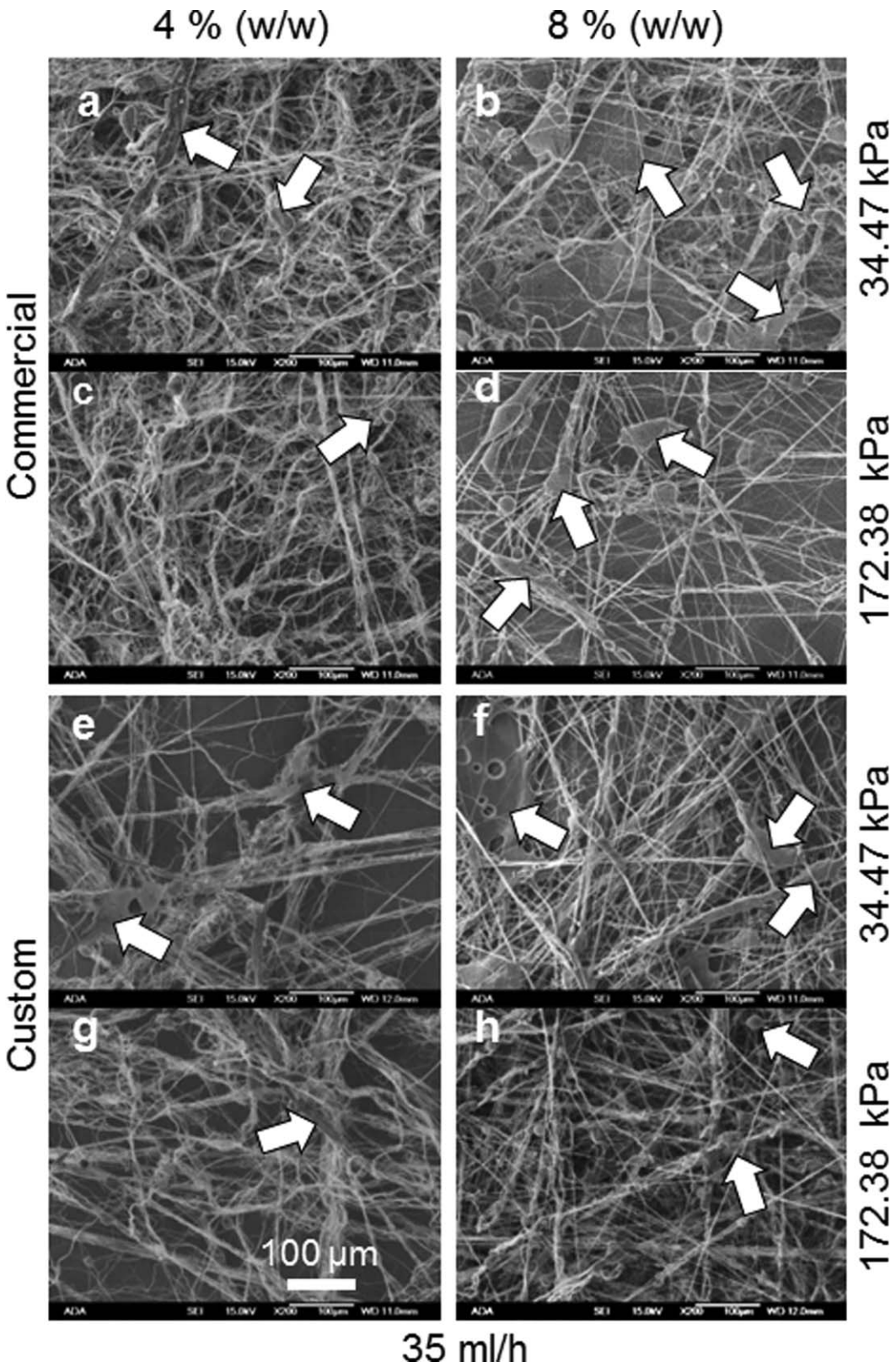

Figure 1. Scanning electron micrographs of the representative samples deposited using commercial (CA, images a–d) and a custom-built airbrushes (CBA, images e–h). The arrows point to unprocessed polymer beads.

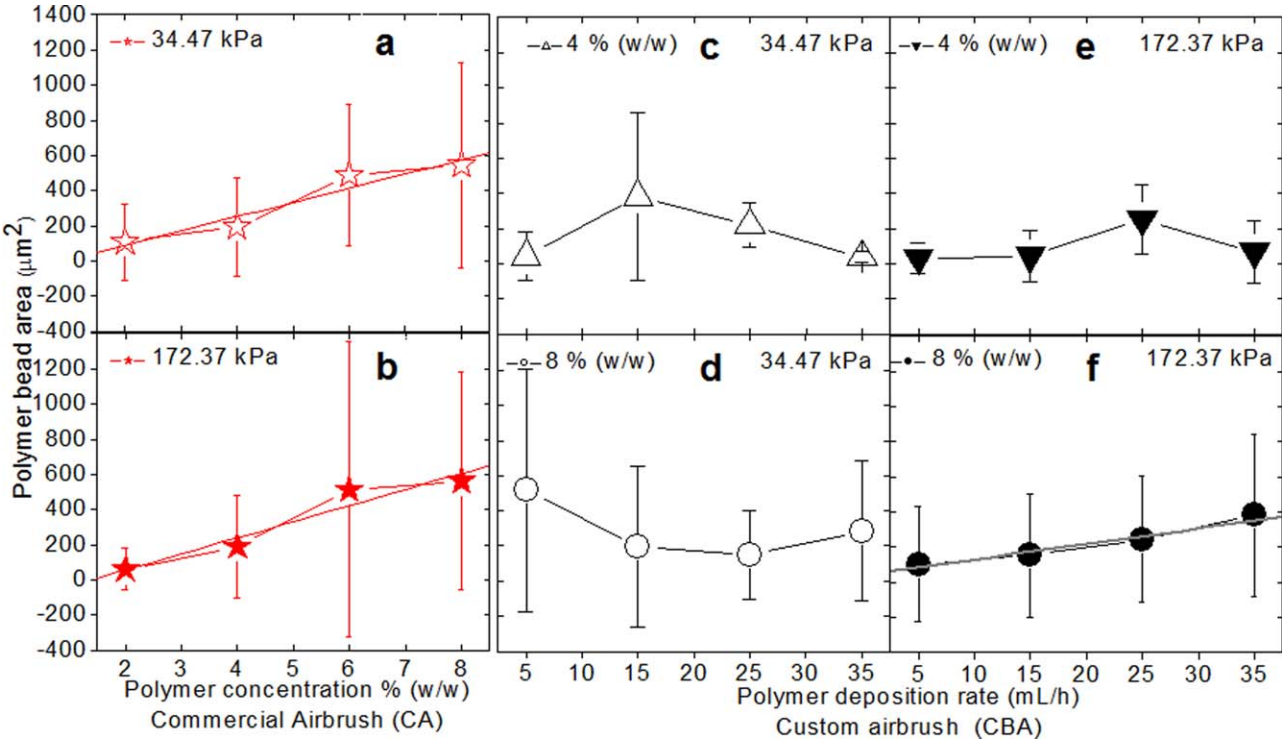

Figure 2. Calculated polymer bead area (mean ± SD) as a function of polymer concentration and air pressure for commercial airbrush (CA, panels a,b) and custom-built airbrush (CBA, panels c–f). "----" indicates the best linear fit. Analysis based on three imaged areas (n = 3). [Color figure can be viewed in the online issue, which is available at wileyonlinelibrary.com.]

deposition rate [$R^2 = 0.74$; $a = -3.73$; Figure 4(e)]. At 8% w/w PCL, a similar trend was observed ($R^2 = 0.73$) at a lower rate [$a = -1.43$; Figure 4(f)]. However, the statistical analysis of the data displayed in Figure 4(a–f) indicated that the numbers of the detected beads in both the CA- and/or CBA-deposited fibers were not statistically different, regardless of the polymer concentration, gas pressure, or brush type used.

Effects of the Gas Pressure, Polymer Concentration, and Device Type on the Polymer Fiber Diameter

The diameter of the fibers synthesized with the CA at 172.37 kPa increased with increasing polymer concentration [$R^2 = 0.96$, $a = 0.19$, Figure 5(b)]. The effect was less pronounced at 34.47 kPa [$R^2 = 0.91$, $a = 0.14$, Figure 5(a)]. At a constant polymer concentration and various pressures, the results were statistically different for only 2 and 4% w/w polymer concentrations ($p < 0.01$). At a constant pressure and various polymer concentrations of 4 and 8% w/w, the differences in the fiber diameters were statistically significant in all cases ($p < 0.001$).

The CBA fiber diameter at 34.47 kPa [Figure 5(d)] appeared to have a better correlation with the deposition rate for 8% w/w with $R^2 = 0.99$ than for fibers deposited at 172.37 kPa with $R^2 = 0.70$ [Figure 5(f)]. The average CA fiber diameter for 4% w/w (at 172.37 kPa) was statistically higher than for the corresponding CBA (at 35 mL/h) samples ($p < 0.001$). A similar relationship was found for the 8% w/w PCL with the CA (at 34.47 kPa) and CBA fibers (at 35 mL/h), $p < 0.05$ [Figure 5(a,c,d)].

More in-depth analysis of the CA-deposited fibers showed that the samples deposited at 4% w/w had a better defined average fiber diameter ($d_{ave} \leq 0.74$ μm) and its distribution [~85% ≤ 1 μm; Figure 6(a,b)] than the 8% w/w PCL samples [Figure 6(c,d)]. Among all of the CA samples, the most defined diameter was found in the samples deposited at the lower polymer concentration of 4% w/w and the higher gas pressure of 172.37 kPa [$d_{ave} = 0.55$); Figure 6(b)]. The highest average diameter was observed in 8% w/w deposited at 172.37 kPa [$d_{ave} = 1.21$ μm; Figure 6(d)]. The analysis of CBA revealed a much smaller average fiber diameter ($d_{ave} \leq 0.18$ μm) and a narrower distribution [~100% ≤ 0.37 μm; Figure 7(a,b)] than was detected for 4% w/w PCL for the 8% w/w specimens ($d_{ave} \leq 0.43$ μm, ~80% ≤ 0.37 μm) at the same gas pressures [Figure 7(c,d)]. The use of the lower PCL concentration seemed to be important for controlling the constant fiber diameter, regardless of the applied gas pressure [Figure 7(a,b)]. The higher PCL concentration (8% w/w) deposited at a greater pressure (172.37 kPa) resulted in more defined fiber diameter ($d_{ave} = 0.25$ μm) and a narrower distribution [~100% ≤ 0.75 μm; Figure 7(d)].

Polymer Solution Viscosity

The viscosities of the PCL/chloroform solutions (Figure 8) showed an excellent correlation ($R^2 = 0.99$) for the given range of polymer concentrations. The values for the polymer solutions with 8% w/w PCL or higher were calculated from the power equation $y = 1.25x^3$.[18] The viscosity data was particularly useful in assessing the quality of the polymer suspension, estimating solution energy and work required to break up the polymer solution to form fibers.

Viscosity results suggested that the PCL/chloroform solution was considered to be well dispersed, entangled, and in the semi-diluted range.[19]

DISCUSSION

The initial analysis of the bead area in the CA-synthesized matrices revealed a strong correlation between the increase in the polymer concentration and the polymer bead area, but no relationship to pressure was found. When we used the CBA (4–8% w/w) and various pressures, no strong correlation to the bead area was detected; the exception was 8% w/w at 172.37 kPa. Generally, the CBA-deposited fibers had a lower average bead area for all of the tested conditions. On the other hand, the number of beads was comparable in both the CA and CBA depositions without any correlation to the polymer PCL concentration, deposition rate, or gas pressure. An exception was found for the CBA deposited at 4 or 8% w/w PCL and at higher gas pressures, where there was a decline in the bead number with increasing deposition rate. In fact, the more negative *a* calculated for the 4% w/w polymer may have suggested a greater contribution of gas energy to effectively break up the polymer solution.

The diameters of the CA-deposited fibers increased with higher polymer concentrations but not with gas pressure. The CBA-synthesized fibers showed practically no correlation with the deposition rate or gas pressure but some dependence on the polymer concentration. The increase in the PCL polymer concentration and the deposition at the highest rate during the use of the CBA resulted in a statistically higher fiber diameter. Similar observations were reported by Oliveira *et al.*[19] The larger fiber diameter was not associated with a higher bead count but rather with a greater bead area. However, when compared against the CA deposition, the control of the fiber diameter appeared to be better in the CA, but it resulted in an increase in the bead size.

When we considered fiber fabrication and the importance of factors as such as the (1) material reproducibility (narrower fiber diameter distribution), (2) matrix quality (smaller number and size of beads), and (3) control of fiber fabrication (polymer feed rate at appropriate gas pressures), the tested brushes seemed to have comparable performance but only at lower polymer concentrations. That was particularly important for CA deposition, which we found to provide comparatively good fiber quality at the tested parameters (4% w/w deposited at 34.47 and 172.37 kPa). However, the fiber quality drastically deteriorated at higher polymer concentrations (8% w/w). Therefore, the results from CBA deposition were more promising because the higher polymer concentration and deposition rates lowered the overall bead size. The observed weak trends suggested that the CBA deposition was more reproducible and efficient when applied at higher PCL polymer concentrations.

The available literature indicates that for designs similar to CBA, polymer solution atomization is thought to be the primary mechanism responsible for fiber formation.[24] Specifically, fibers are synthesized when droplets of polymer solution break off from the main jet and are extruded into filaments by aerodynamic forces. In the context of the data presented here, one should, therefore, find the area covered by polymer beads to be independent of the polymer feed rate (for polymer feed rates significantly less than the volumetric flow rate of the gas). However, our results show that for CBA, the polymer bead area was dependent on the polymer feed rate. It was then likely that the fibers were not created in flight, but rather they formed as filaments and later detached from the jet. An analysis of the time evolution of polymer concentration due to evaporation indicated that when single fibers broke off, at least some fraction was still in liquid form. It was, therefore, likely that a first-wind capillary pinching of the liquid filaments governed fiber fabrication.

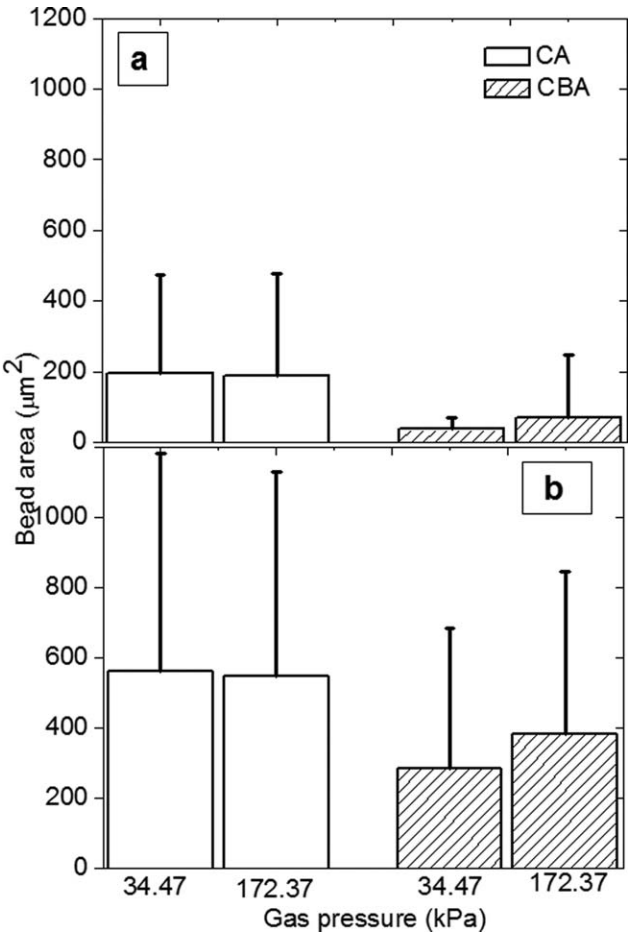

Figure 3. Comparison of the average bead area (mean ± SD) deposited at 34.47 and 172.37 kPa by CA and CBA at 4% (w/w) (panel a) and 8% (w/w) (panel b). Analysis based on three imaged areas (n = 3).

On the basis of the measured fiber diameters (Figures 6 and 7), we were able to calculate the energy required to pinch off a liquid filament to form a fiber. First, we considered the polymer solution to be a micelle in pure chloroform to calculate the surface tension from the difference in the chemical potentials between the solution and a pure solvent with the Gibbs absorption theorem.[28] A Langmuir isotherm was used to estimate the surface excess concentration of the polymer.[29] The filament radius (r) was expressed in terms of the fiber radius with the following equation:

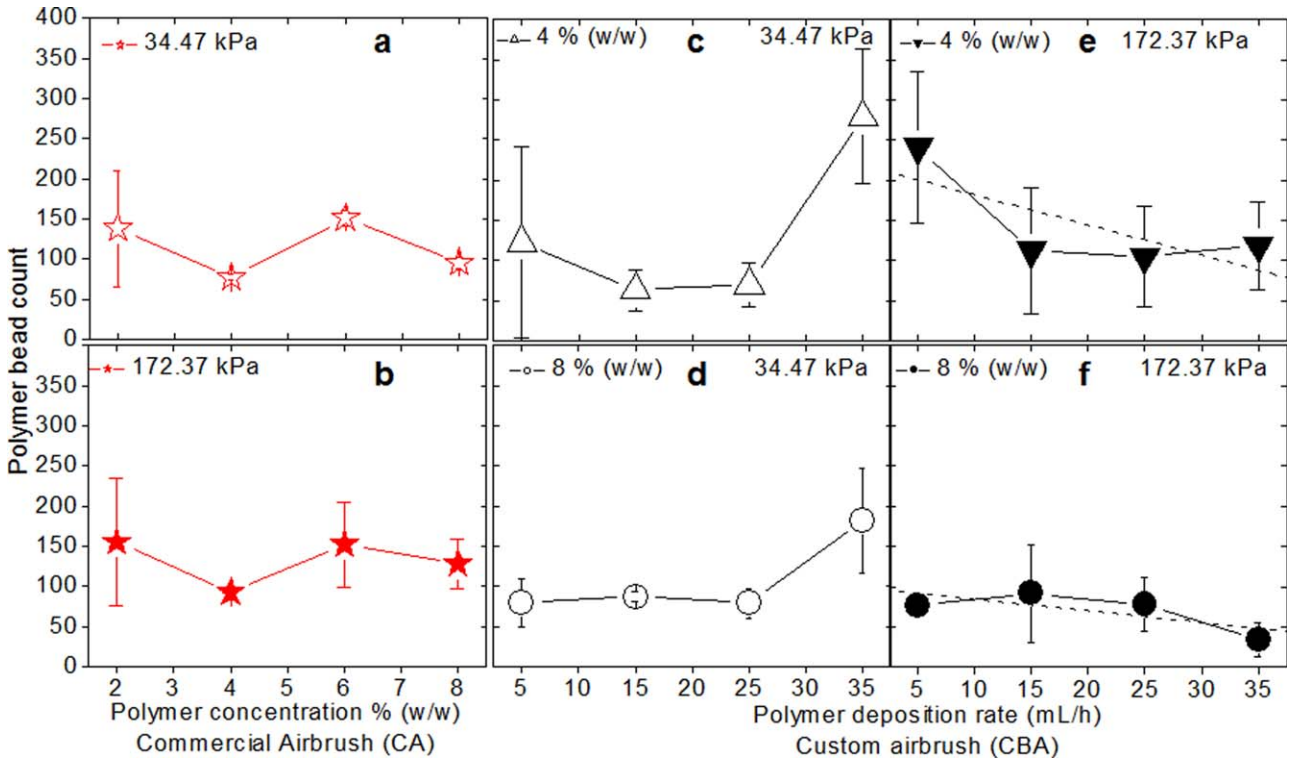

Figure 4. Polymer bead count (mean ± SD) as a function of polymer concentration, air pressure (CA, panels a,b) and polymer deposition rate (CBA, panel c–f). "----" indicates the best linear fit. Analysis based on three imaged areas (n = 3). [Color figure can be viewed in the online issue, which is available at wileyonlinelibrary.com.]

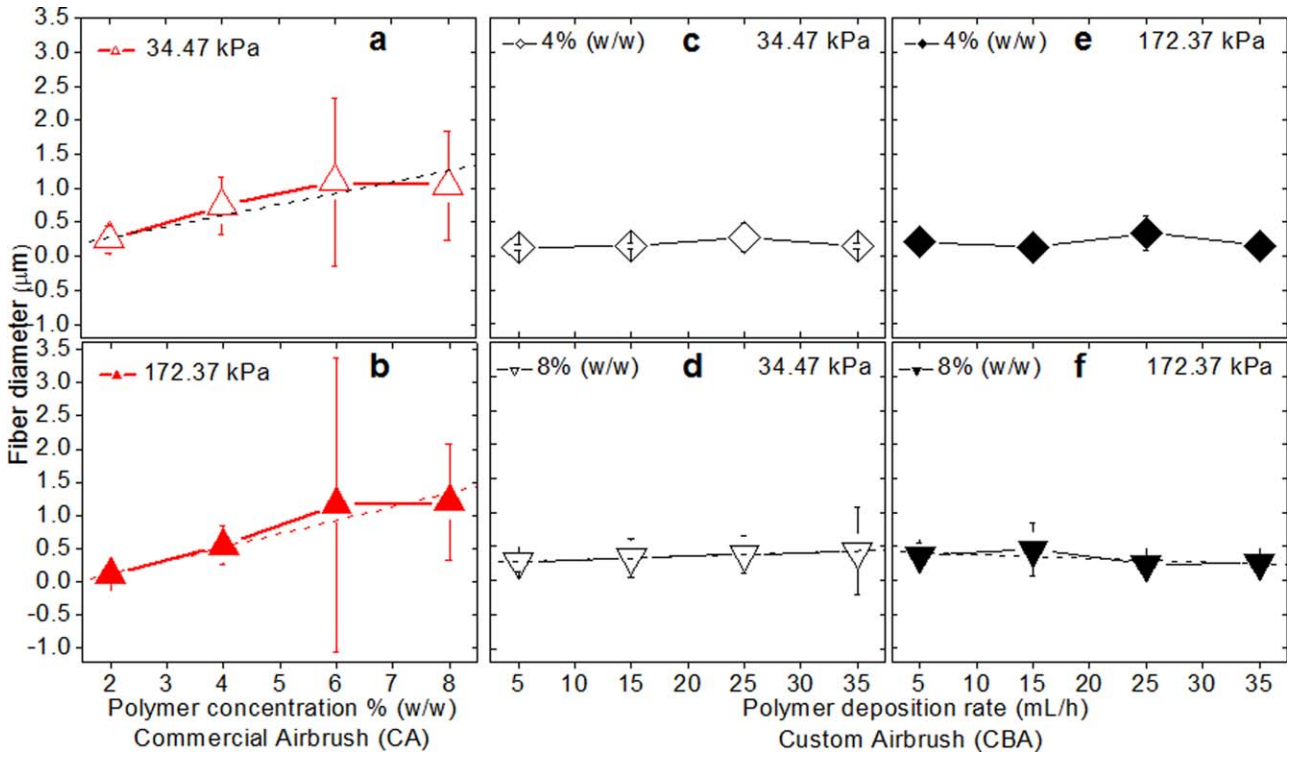

Figure 5. Fiber diameter (mean ± SD) as a function of polymer concentration, gas pressure (CA, panel a,b) and polymer deposition rate (CBA, panel c–f)."----" indicates the best linear fit. Analysis based on three imaged areas (n = 3). [Color figure can be viewed in the online issue, which is available at wileyonlinelibrary.com.]

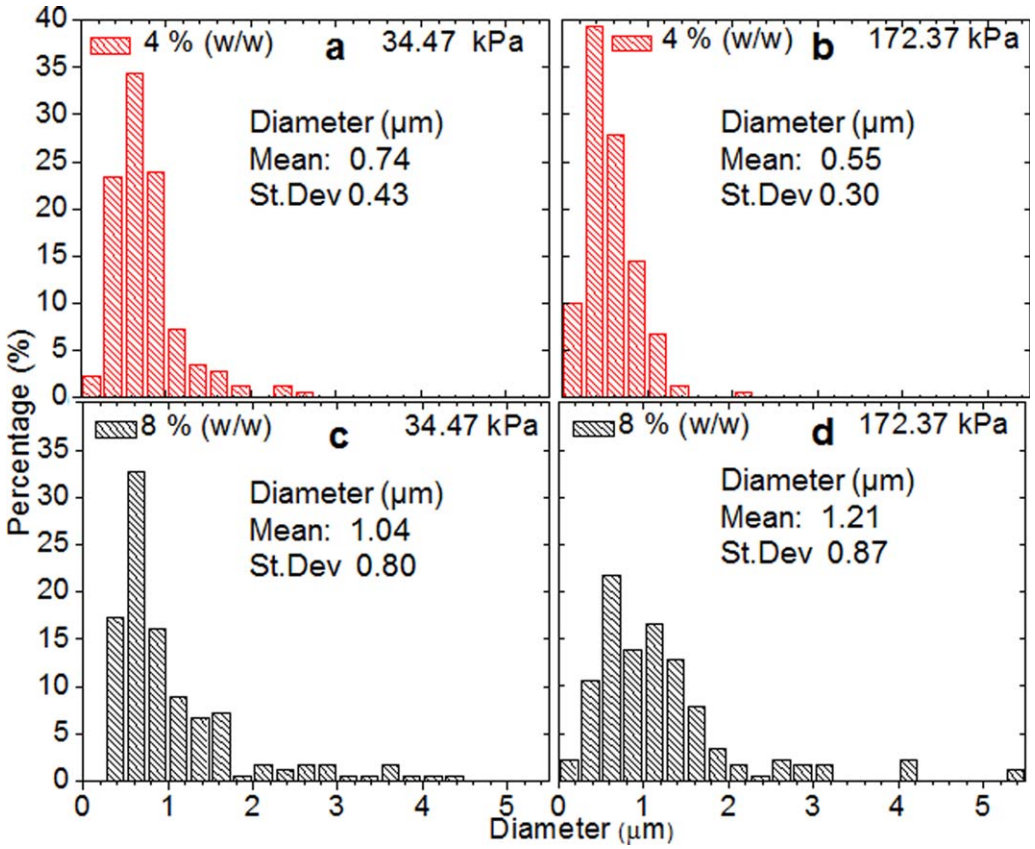

Figure 6. Histograms of fiber diameter deposited at 4% (w/w) using CA (panel a,b) and 8% (w/w), panel c,d. Effect of low, 34.47 kPa, (panel a,c) and high, 172.37 kPa, (panel b,d) gas pressures on fiber diameter distribution. Analysis based on three imaged areas (n = 3). Calculated mean and SD for each tested condition are listed in each panel. [Color figure can be viewed in the online issue, which is available at wileyonlinelibrary.com.]

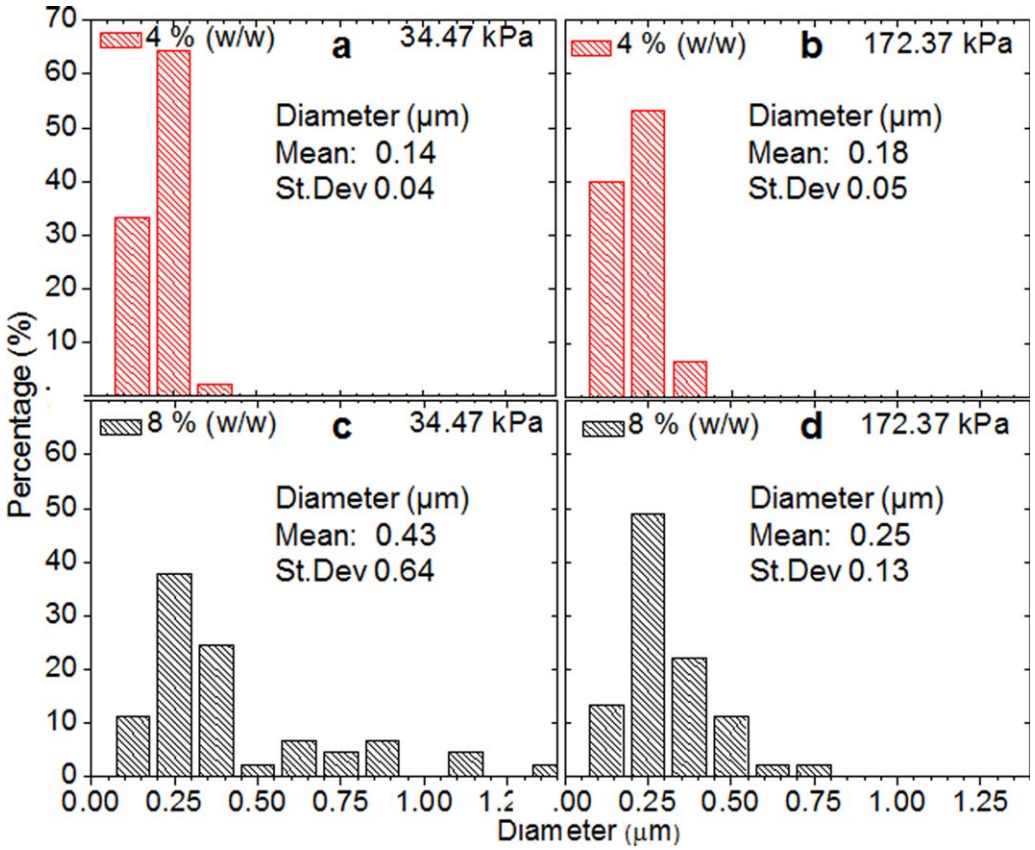

Figure 7. Histograms of fiber diameter deposited at 4% (w/w) using CBA (panel a,b) and 8% (w/w), panel c,d. Effect of low, 34.47 kPa, (panel a,c) and high, 172.37 kPa, (panel b,d) gas pressures on fiber diameter distribution. Analysis based on three imaged areas (n = 3). Calculated mean and SD for each tested condition are listed in each panel. [Color figure can be viewed in the online issue, which is available at wileyonlinelibrary.com.]

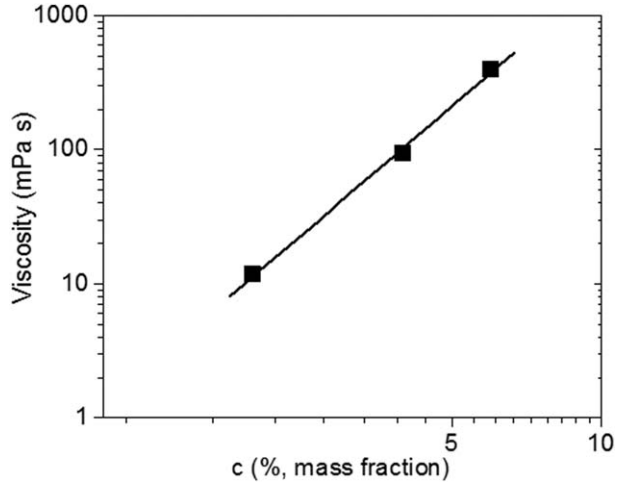

Figure 8. Analysis of viscosities of PCL-chloroform solutions with increasing PCL concentrations at room temperature.

$$r=\sqrt{\frac{\rho_f}{c'\rho*}}z$$

where z is the fiber radius, ρ_f is the fiber density, ρ^* is the filament density, and c' is fractional of c, where c is defined as (%, mass fraction). These expressions were then used to calculate the surface energy of a liquid cylinder (E):

$$E=2\pi rl\sigma$$

where l is the length of a liquid cylinder representing the fibers and σ corresponds to polymer and solvent surface tension. This gave the concentration-dependent pinching energy [$E_p(c)$]:[27,30,31]

$$E_p(c)=20\sqrt{\frac{\rho_f}{c\rho*}}\pi lz\sigma(c)$$

As $c \rightarrow 0$, so does z; thus, $E_p(0) < \infty$. The calculated pinching energies (Figure 9) indicated that the CBA design required lower energies to form fibers than the CA did for all polymer concentrations, except for 2% w/w. Our analysis suggested that CBA designed synthesized fibers more efficiently.

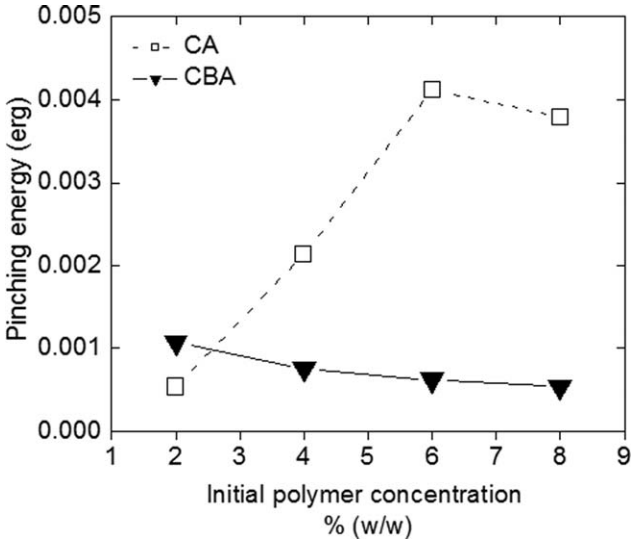

Figure 9. Calculated pinching energies required to form fibers (at 172.37 kPa) for CA and CBA (at 35 mL/h polymer feed rate) devices.

The details of the time-dependent fabrication analysis were beyond the scope of this study and will be explained in a follow-up publication.

Although the fiber formation efficacy was defined by the polymer solution characteristics, our results suggest that the brush design and its ability to break up the polymer solution stream is also very important. Features like the nozzle design and control over the feed rate appear to have a great impact on the fiber formation and quality.

The tested commercial brush did not have the proper nozzle dimensions and lacked control over the polymer feed rate; this resulted in more energy-intensive (larger fiber diameters) and less optimal fiber formation (larger polymer beads) at higher polymer concentrations.

CONCLUSIONS

Compared to the CA, the CBA apparently broke up the PCL/chloroform solution more efficiently by delivering fibers with a narrower diameter distribution and smaller polymer beads. For both the CA and CBA, the bead number was unaffected by the pressure, polymer concentration, and deposition rate. Also, for both devices, solutions with a lower polymer concentration broke up more easily and formed smaller beads and finer fibers. At higher pressures, the CBA device more effectively broke up the concentrated polymer solutions and delivered smaller diameter fibers when compared to the CA. More efficient polymer solution breakup by a capillary pinching mechanism allowed the CBA to form better quality fibers. Our study highlights the importance of proper brush design and its effect on fiber fabrication and fiber matrix quality.

ACKNOWLEDGMENTS

The authors thank S. Hudson (National Institute of Standards and Technology) for performing the polymer viscosity measurements and D. Skrtic for his insightful comments, discussions, and corrections of the article. The authors also thank G. Duppins and K. Hoffman for their help in improving the article. They also acknowledge the financial support of the ADA Foundation.

The authors declare no competing financial interests.

Certain commercial materials and equipment were identified or used in this research for adequate execution of the experimental procedure. In no instance does such identification imply recommendation or endorsement by the ADA Foundation or National Institute of Standards and Technology that the material or equipment is necessarily the best available for the purpose.

One of the authors (W.T.) conceived the idea, performed the experiments, analyzed the data, and wrote/edited the article. One of the authors (X.-L.P.) performed experiments and helped analyze the data. Two of the authors (G.G. and C.M.) performed the simulations, analyzed the data, and wrote and edited the article.

REFERENCES

1. Breuer, O.; Sundararaj, U. *Polym. Compos.* **2004**, *25*, 630.
2. Smook, J.; Torfs, J.; Van Hutten, P.; Pennings, A. *Polym. Bull.* **1980**, *2*, 293.
3. Shen, S.; Henry, A.; Tong, J.; Zheng, R.; Chen, G. *Nat. Nanotechnol.* **2010**, *5*, 251.
4. Chen, Y.-M.; Ting, J.-M. *Carbon* **2002**, *40*, 359.
5. Sundaray, B.; Subramanian, V.; Natarajan, T.; Krishnamurthy, K. *Appl. Phys. Lett.* **2006**, *88*, 143114.
6. Cai, Z.; Martin, C. *J. Am. Chem. Soc.* **1989**, *111*, 4138.
7. Pinto, N.; Johnson, A., Jr.; MacDiarmid, A.; Mueller, C.; Theofylaktos, N.; Robinson, D.; Miranda, F. *Appl. Phys. Lett.* **2003**, *83*, 4244.
8. Babel, A.; Li, D.; Xia, Y.; Jenekhe, S. *Macromolecules* **2005**, *38*, 4705.
9. Li, W.; Laurencin, C.; Caterson, E.; Tuan, R.; Ko, F. *J. Biomed. Mater. Res.* **2002**, *60*, 613.
10. Tutak, W.; Sarkar, S.; Lin-Gibson, S.; Farooque, T.; Jyotsnendu, G.; Wang, D.; Kohn, J.; Bolikal, D.; Simon, C. *Biomaterials* **2013**, *34*, 2389.
11. Brink, L.; Elbers, S.; Robbertsen, T.; Both, P. *J. Membr. Sci.* **1993**, *76*, 281.
12. Salonen, P.; Rahmat-Samii, Y.; Schaffrath, M.; Kivikoski, M. *IEEE* **2004**, *1*, 459.
13. Gibson, P.; Schreuder-Gibson, H.; Rivin, D. *Colloids Surf. A* **2001**, *187*, 469.
14. Carnell, L.; Siochi, E.; Holloway, N.; Stephens, R.; Rhim, C.; Niklason, L.; Clark, R. *Macromolecules* **2008**, *41*, 5345.
15. Gibson, P.; Schreuder-Gibson, H.; Rivin, D. *AIChE J.* **1999**, *45*, 190.
16. Kim, P.; Shi, L.; Majumdar, A.; McEuen, P. *Phys. B* **2002**, *323*, 67.
17. Behrens, A.; Casey, B.; Sikorski, M.; Wu, K.; Tutak, W.; Sandler, A.; Kofinas, P. *ACS Macro Lett.* **2014**, *3*, 249.
18. Srinivasan, S.; Chhatre, S.; Mabry, J.; Cohen, R.; McKinley, G. *Polymer* **2011**, *52*, 3209.
19. Oliveira, J.; Moraes, E.; Costa, R.; Afonso, A.; Mattoso, L.; Orts, W.; Medeiros, E. *J. Appl. Polym. Sci.* **2011**, *122*, 3396.
20. Medeiros, E.; Glenn, G.; Klamczynski, A.; Orts, W.; Mattoso, L. *J. Appl. Polym. Sci.* **2009**, *113*, 2322.
21. Marsh, K.; Marsh, K. Recommended Reference Materials for the Realization of Physicochemical Properties; Blackwell Scientific Publications: Oxford, United Kingdom, **1987**.
22. Park, S.; Lim, J.-H.; Chung, S.-W.; Mirkin, C. *Science* **2004**, *303*, 348.
23. Hoffman, K.; Skrtic, D.; Sun, J.; Tutak, W. *Tissue Eng. C* **2014**, *21*, 284.
24. Lu, B.; He, Y.; Duan, H.; Zhang, Y.; Li, X.; Zhu, C.; Xie, E. *Nanoscale* **2012**, *4*, 1003.
25. Hudson, D.; Sarangapani, P.; Pathak, J.; Migler, K. *J. Pharm. Sci.* **2014**.
26. Bruin, J. "Newtest: command to compute new test." UCLA Academic Technology Services, Statistical Consulting Group: **2006**. Available at: http://www.ats.ucla.edu/stat/gpower/indepsamps.htm
27. Tomotika, S. *Proc. R. Soc. London Ser. A* **1935**, *150*, 322.
28. Rosen, M. J. Adsorption of surface-active agents at interfaces, the electrical double layer. Surfactants and Interfacial Phenomena, 3rd ed.; Wiley: Hoboken, NJ, **2004**; p 34.
29. Bell, C.; Breward, C.; Howell, P.; Penfold, J.; Thomas, R. *Langmuir* **2007**, *23*, 6042.
30. Hsu, C.-M. Master's Thesis, Worcester Polytechnic Institute, **2003**.
31. Deitzel, J.; Kleinmeyer, J.; Harris, D.; Beck Tan, N. *Polymer* **2001**, *42*, 261.